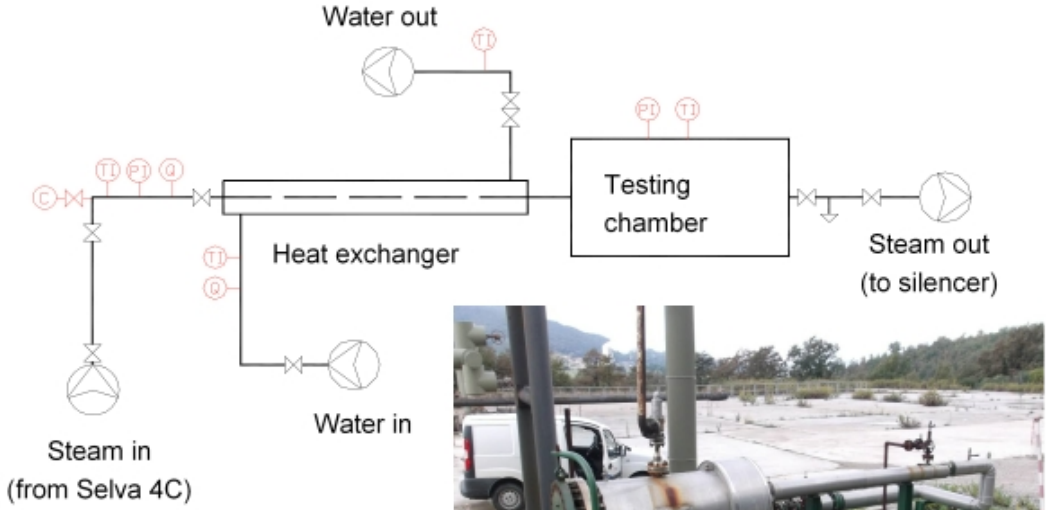
Water out
Testing chamber
Heat exchanger
Steam out (to silencer)
Water in
Steam in (from Selva 4C)

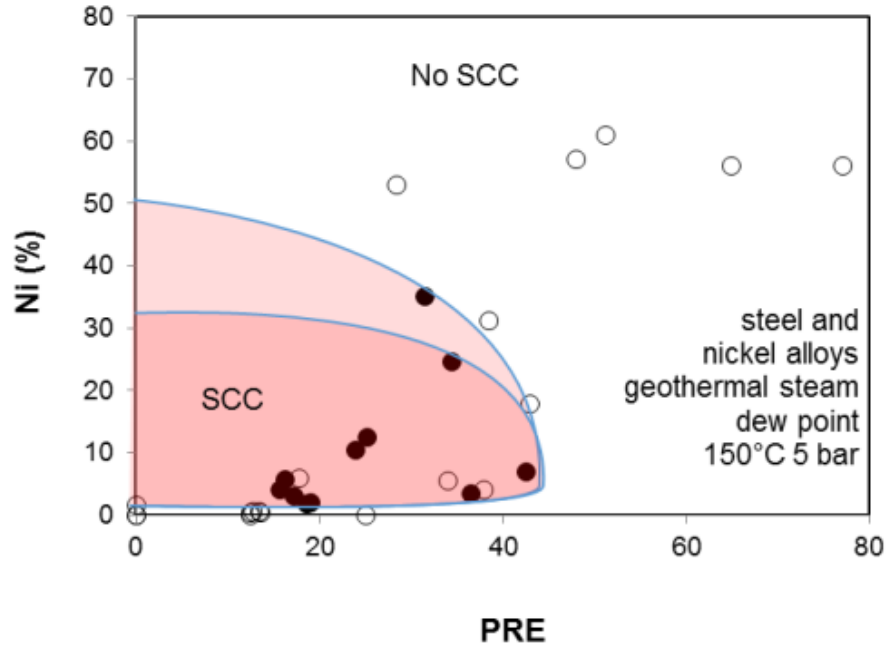
No SCC
SCC
steel and nickel alloys geothermal steam dew point 150°C 5 bar
Ni (%)
PRE

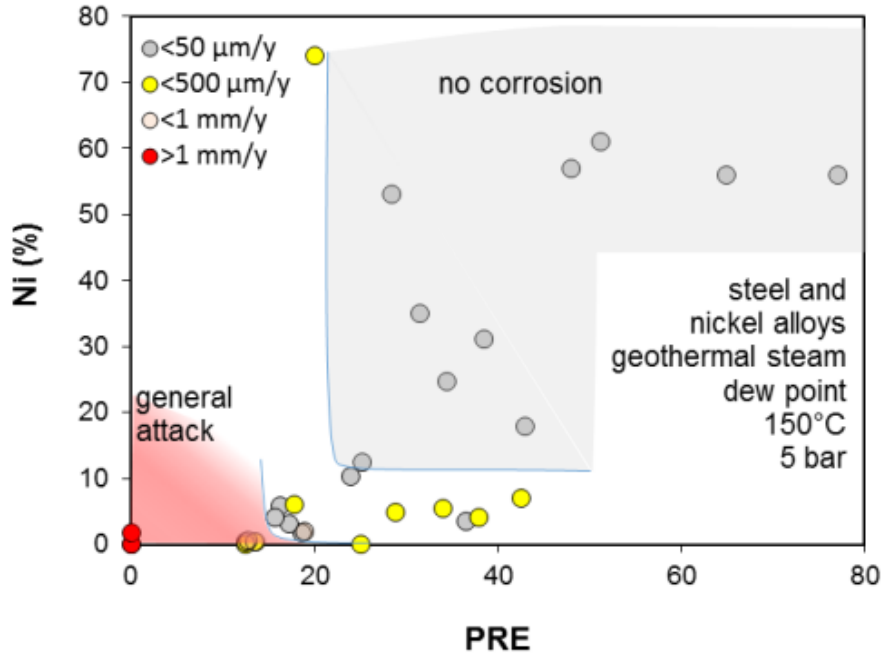
<50 µm/y
<500 µm/y
<1 mm/y
>1 mm/y
no corrosion
general attack
steel and nickel alloys geothermal steam dew point 150°C 5 bar
Ni (%)
PRE

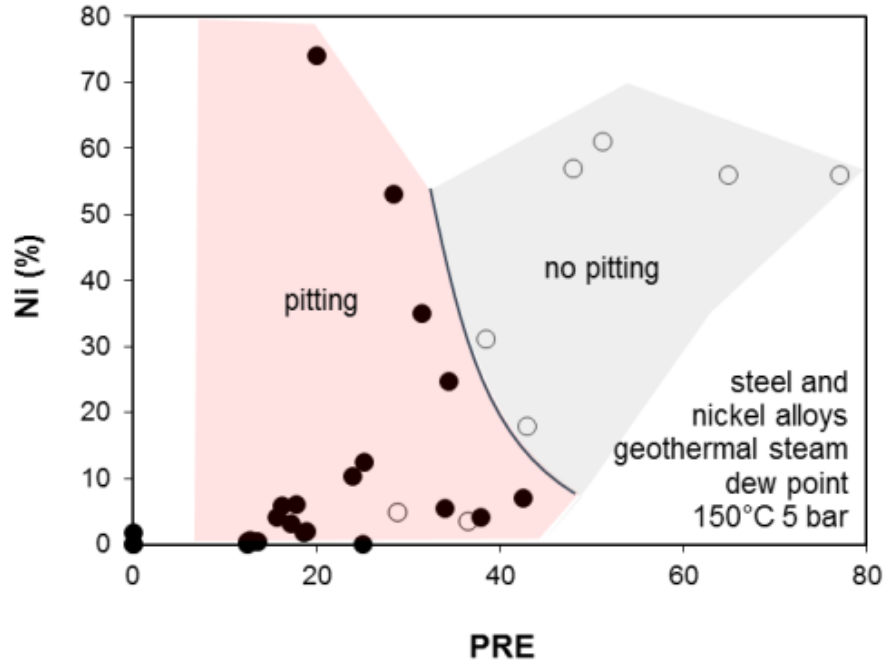
pitting
no pitting
steel and nickel alloys geothermal steam dew point 150°C 5 bar
Ni (%)
PRE

Materials selection for dew-point corrosion in geothermal fluids containing acid chloride

M. Cabrini, S. Lorenzi, T. Pastore, Università di Bergamo, Bergamo, Italia
M. Favilla, R. Perini. B. Tarquini, Enel, Larderello, Italia

Abstract

The paper is aimed to the evaluation of the corrosion behavior of corrosion resisting alloys (CRAs) in geothermal fluids operating at the dew point.
Several test series were carried out in geothermal production sites of Tuscany (Italy) under continuous flow. The vapor was extracted directly from the main flow and it was conveyed in an experimental device designed to simulate dew point conditions.
Nine martensitic stainless steel, one precipitation hardening stainless steel with martensitic structure, two ferritic extra low interstitial (ELI) stainless steels, four duplex (austenitic-ferritic) stainless steel, five austenitic stainless steels, six nickel alloys/super austenitic stainless steels, four titanium alloys were tested.
The main forms of corrosion were general corrosion, localized corrosion (pitting and crevice) and stress corrosion cracking. Corrosion maps are presented as a function of PREN index, chromium, molybdenum and nickel content.

Key words

Dew Point Corrosion, Stainless Steels, Nickel Alloys, Titanium Alloys, Geothermal Fluids, Acid Chlorides, Stress Corrosion Cracking, Localized Corrosion

1 Introduction

The presence of acid chlorides in steam - mainly hydrogen chloride (HCl) and ammonium chloride (NH_4Cl) - promotes severe corrosion in geothermal power plants. In the vapor-dominated system of Larderello, risk of localized corrosion and stress corrosion cracking arises on corrosion resistant alloys (CRA) blades of the wet section of steam turbines. Furthermore, severe general corrosion can be noticed in cold zones of carbon steel pipelines conveying steam from wells to turbines [1] [2] [3] [4].
At the dew point, that usually is in the range between 150 and 190°C at the operational pressure of plants, the early stage of condensation promotes the formation of a layer of very aggressive saline solution with acid pH, ranging between 2 and 4. Very high chloride concentrations in the order of 20000 ppm were estimated, depending on the chloride content in the vapor phase. Relevant concentrations of ammonium ion and boric acid were also detected.
Nowadays, corrosion mitigation is mainly achieved through steam scrubbing systems and chloride abatement with alkaline sodium hydroxide solution [5] [6] [7] [8] [9]. Besides an increase in operating costs, such treatment reduces the fluid temperature leading to relevant loss of power of about 0.5 MW on 15 MW turbine. Thus, the use of CRAs can be a suitable solution [10].

Corrosion damages on turbine blades operating at dew point are mainly due to general corrosion of low-alloyed steels, localized corrosion (pitting and under deposit crevice attack), stress corrosion cracking and corrosion-erosion. In addition, rotor blade collapse under cyclic loading at frequency higher than 50 Hz can occur due to fatigue crack initiation and propagation from pitting and stress corrosion.
Materials selection guidelines for acid chloride service in geothermal turbines mainly recommend the use of stainless steels and nickel alloys with a high content of chromium and molybdenum, but they are very expensive. However, titanium alloys should also be taken into account due to both cost and performances. Thomas [11] discussed their application for geothermal service as viable candidates to replace common stainless steels in very aggressive environments. In addition, several advantages in terms of decrease of the weight of components and axial loads on rotating blades can be evidenced.
Furthermore, the reduction of loads on rotor blades allows the use of alloy with mechanical strength below the level required for iron alloys and nickel alloys.
Based on these considerations, extensive researches were made in the early 80s on two geothermal sites during different campaigns to perform an experimental evaluation of corrosion resistance of different alloys. The experimental tests were mainly performed in situ, under real dew point exposure conditions. Recently, Yang et al [12] still outlined that it is recommend to study dew point corrosion by in situ test method owing to the different mechanisms involved with respect to acid solutions.
Initially, the research was aimed to identify the best technical-economic solution for the construction of standardized turbines. The testing was then addressed to identify materials for blades operating in contact with geothermal vapor containing up to 10 ppm of acid chloride. The results of exposure tests are discussed and analyzed in order to attain suitable design criteria in terms of material selection of materials operating at the dew point in geothermal plants.

2 Experimental

2.1 Testing section and environmental conditions

The investigation was performed in sections specifically designed for corrosion testing in two geothermal sites. Table 1 describes the typical fluid compositions at testing sections inlet. Tests have been performed at the dew point, at about 150°C and 5 bar pressure, with vapor quality above 0.9 for 30 days. Four similar testing devices were built. Two test sections were installed in the Geothermal Plant of San Martino during ‘80s and ‘90s, and the other two sections were placed at the Selva 4 C well since 2000.

Table 1: composition of geothermal fluids

Plants	S. Martino	Selva 4C
Not condensable gases (%)	2.13	4.97
pH	6.1	5.5
CO_2 (%w)	87.75	91.19
H_2S (%w)	2.36	1.72
H_3BO_3 (ppm)	501	1106
Cl^- (ppm)	51.5	102
NH_4^+ (ppm)	56	69.7
Na^+ (ppm)	0.1	0.01

Figure 1 shows the layout of the experimental device. Steam from the main vapor line is conveyed to the test section and temperature and pressure were adjusted by means of a laminating valve and a heat exchanger in order to achieve incipient condensation conditions into the testing chamber. A further back pressure valve installed at the output of the testing chamber stabilizes the temperature and pressure. A conical joint was installed at the inlet to avoid turbulence and homogenize the flow. Finally, the steam is discharged passing through demister and silencer.
The testing device was equipped with pressure and temperature sensors for environmental condition monitoring. The specimens were fixed into the chamber by means of metallic plate. Insulating gaskets were used in order to avoid galvanic coupling between different metals. The specimens were placed at different distances from the steam ingress. During all tests, two specimens of AISI 316 stainless steel were exposed for comparison purposes in order to verify that aggressive conditions were effectively achieved. In such conditions, AISI 316 stainless steel is susceptible to chloride stress corrosion cracking.

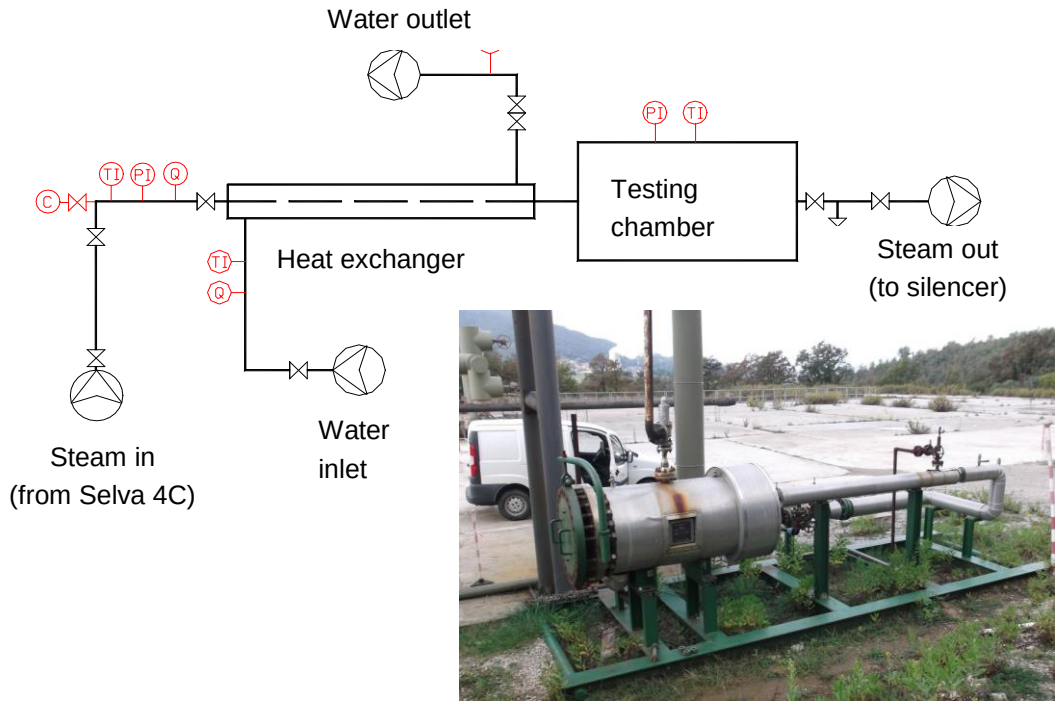

Figure 1: experimental station at Selva 4 C plant and layout of testing section

2.2 Specimens

Weight loss measurements were also performed on 100x20 mm specimens with an hole for mounting. The measurements were carried out by means of 0.1 mg precision scale, U-bend specimens (100x10x3mm) were used to perform SCC tests (Figure 2). The thickness was around 3 mm for most of the specimens. Slightly thicker specimens were used in function of metal sheet thickness availability. The surfaces were polished by means of emery paper up to 1000 grit and then they were degreased in acetone.
After exposure, the corrosion scale was removed by pickling in 5% hydrochloric acid with hexamethylenetetramine. The corrosion morphology was analyzed through micro and macro observations of the surfaces and on the metallographic sections of the U-bend specimens for detecting SCC.

2.3 Materials

Several materials were tested including martensitic, ferritic, austenitic and duplex stainless steels, nickel super alloys, and titanium alloys having different resistance to localized corrosion and chloride stress corrosion cracking. Table 2 summarizes their compositions. The stainless steels and nickel alloys have chromium contents between 12 and 27 %, molybdenum up to 17% and nickel up to 74%. Furthermore, there are two traditional Ti6Al4V (grade 5) alloys, a low interstitial Ti Grade 29 ELI alloy with ruthenium and Ti 6246 alloy. The materials were tested in as received metallurgical conditions.

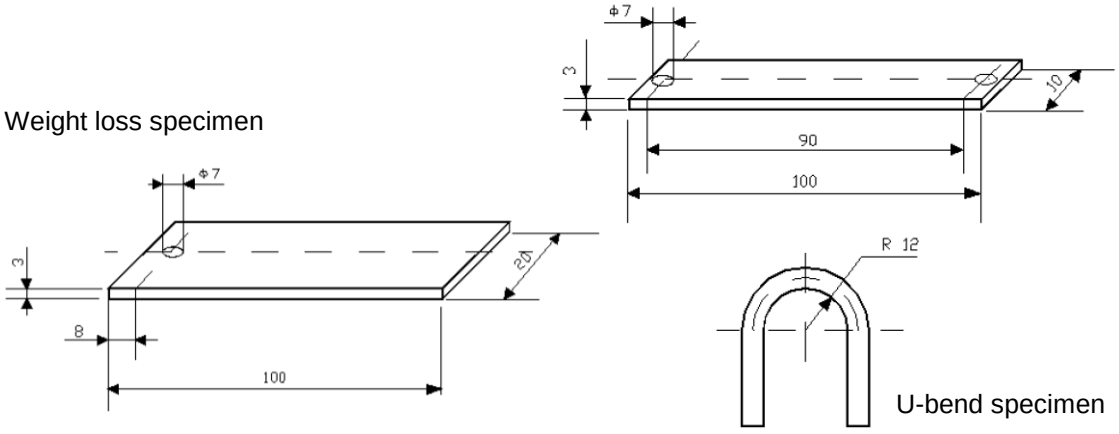

Figure 2: dimensions of specimens

3 Results and discussion

3.1 Dew point solution

At the pressure of the vapor in the inlet section of the turbine, the mean value of the temperature at dew point is 190 °C. However, such temperature decreases to 150-160 °C due to the pressure drop inside the turbine.

The composition of the solutions at the dew point was estimated by means of ENEL proprietary software (LAVAG code) [2] by using the thermochemical data of fluids of the Larderello plants.

The composition of the first droplet was calculated by considering the thermodynamic conditions of the fluid, the average chemical composition of steam, and the adiabatic transformation that occurs during steam expansion inside the turbine. Table 3 shows the chemical composition estimated for both the sites, San Martino and Selva 4C. The composition of the first droplet shows very low pH - between 3.8 and 3.9 - and very high chloride and boric acid contents. Hydrogen chloride and ammonium chloride mainly address the low pH values because the ammonia content in the vapor is not sufficient to maintain the pH of solution at neutral point. Ammonium chloride also raises the ebullition temperature allowing condensation at higher temperatures due to the increase of salinity. This phenomenon is almost negligible during isobaric cooling but is relatively important in the case of adiabatic expansion.

Table 2: chemical composition of alloys

Martensitic stainless steels	PRE	Ni	Mn	Cr	Mo	Cu	N	Nb	V
X 15Cr13 Gr. 31	12.6	0.31	0.49	12.3	0.07				
X12CrMo13	13.6	0.31	0.47	11.9	0.52	0.1			
X12Cr13	12.5	<0.75	<1.5	12.5	0				
AISI 403 mod.	13.4	0.47	0.56	11.8	0.5	0.08			
XG 15 Cr 13	12.7	0.6	0.59	12.7					
X14CrNi 19 UNI 6901	18.7	1.82	0.78	18.7					
19Cr 2 Ni	19	2		19					
X15CrNiMo13	17.2	3.1	0.88	11.3	1.8		0.034		0.29
X5CrNiMo126	16.3	5.79	0.56	11.5	1.5	0.2			
X5 CrNiMo12-6	17.8	6	0.6	12.5	1.6	≤0.25			
17-4 PH (AISI 630)	15.8	4.15	0.3	15.8		3.3		0.26	

Ferritic stainless steels	PRE	Ni	Ti	Mn	Cr	Mo	N
NU ELI-T 18-2	25.0		0.44	0.35	17.8	2.2	0.017
NU MONIT 25-4-4	38.0	4.03	0.37	0.34	25	3.93	0.02

Duplex stainless steels	PRE	Ni	Mn	Cr	Mo	N
X3CrMnNiMoN 25-6-4	36.5	3.5	5.63	25.6	2.1	0.25
3 RE 60	28.9	4.94	1.56	18.4	2.8	0.077
SAF 2205	34.1	5.4	1.38	21.8	3	0.15
SUPERDUPLEX	42.5	7		25	4	0.27

Austenitic stainless steels	PRE	Ni	Mn	Cr	Mo	Cu	N
ASTM A 240 Tp. 316	23.9	10.4	1.6	16.4	2.3		
AISI 316	25.3	12.5	<2	17	2.5		
254 SMO	43.0	17.9	0.5	20.2	6.0	0.69	0.18
254 SLX	34.5	24.7	1.49	19.9	4.4	1.45	
Sanicro 28	38.5	31.1	1.41	26.7	3.4	1	0.035

Nichel alloys	PRE	Fe	Ni	Ti	Mn	Cr	Mo	Cu	Al	Nb	V	W	Co
AF 935	31	R	35	2		20	3.5	1.5		0.3			
INCONEL 718	28.4	18	53	0.8		18.5	3			5			
HASTELLOY C22 HS	77.1	<2	56		<0.8	21	17		<0.5			<1	<1
HASTELLOY C22	64.9	3	56		<0.5	22	13				<0.35	3	<2.5
INCONEL 725	48.0	R	57	1.35		20.8	8.3			3.4			
INCONEL 625	51.2	3	61			21.5	9			3			
NIMONIC 80	20	<1.5	74	2.2		20	0		1.3				2

Titanium alloys	Fe	Mo	Al	N	Zr	O	V	Sn	Ru
Ti6Al4V (grade 5)	0,12		6,5	0,008		0,17	4,1		
Ti6Al4V (grade 5)	0,16		6,4	0,011		0,14	4		
Ti 6246	<0,15	6	6	<0,04	4	<0,15		2	
Ti Grade 29	<0,25		6	<0,03		<0,13	4		0,11

Table 3: composition of geothermal fluids estimated at the dew point

Plants	Selva 4C	S. Martino
pH	3.4	3.8
HCO_3^- (ppm)	0.0407	0.14
HS^- (ppm)	0.0025	0.01
H_3BO_3 (ppm)	63745	77958
Cl^- (ppm)	6900	6590
NH_4^+ (ppm)	3600	3438

The partial pressures of CO_2 and H_2S is equal to 0.745 bar and 0.018 bar, respectively. Such conditions classify the environment as sour. However, low risks of sulfide stress corrosion cracking was recognized only on ferritic or martensitic steel blades operating at low temperatures.

3.2 Corrosion forms

The main forms of corrosion identified during testing were general corrosion, pitting corrosion and stress corrosion cracking. In fact, tests were performed under static loading at flow rates not critical for erosion. Furthermore, no formation of deposits on the surface of specimens was noticed due to vapor flow and relatively short exposure time.

3.3 Weight loss

The corrosivity of the environment in terms of general corrosion is primarily related to the acid nature of the condensate that forms at dew point. Corrosion process occurs due to the cathodic process of hydrogen evolution and is favored by both acidity and chlorides, which make passivity film less stable and prevent its reformation on corrosion resistant alloys.
The resistance to this form of attack depends on the alloy composition and microstructure. For stainless steels and nickel alloys the resistance to general corrosion is mainly related to chromium and molybdenum content, that promote the formation of very protective film. In particular, molybdenum can stabilize the film in very acidic environments, characterized by high chlorides content. Thus, it is normally present in the alloys exposed to solutions containing hydrochloric acid.
In order to consider the combined effect of two elements, weight loss of iron and nickel-based alloys were related to PRE (Pitting Resistance Equivalent) number and nickel content. PRE (see also paragraph 3.2) is assumed as stability index of the film and it is calculated by using the following relationship for super-austenitic and duplex stainless steels

$$\mathrm{PRE} = \%\mathrm{Cr} + 3.3 \cdot \%\mathrm{Mo} + 16 \cdot \%\mathrm{N} \quad (1)$$

For traditional austenitic stainless steel grades, martensitic and ferritic stainless steels and nickel alloys, only chromium and molybdenum contents are considered, due to the detrimental effect determined by the precipitation of nitrides.
Nickel modifies the structure of the alloys, balancing ferrite-stabilizing elements as chromium and molybdenum.
Figure 3 shows the weight loss as a function of PRE and nickel content. Three corrosivity classes were considered, such as low, medium, high or very high in function of the corrosion rates. Carbon and low-alloy steels have active behavior, with very high corrosion rates.
Adequate contents of chromium and molybdenum allow the formation of a passivity film, which substantially hinders the generalized corrosion. Thus, the weight loss becomes negligible for austenitic alloys with nickel content above 10% and PRE above 20, whereas it is still appreciable on alloys with low PRE due to the occurrence of pitting attack (Figure 3).
Martensitic and ferritic steels show a corrosion rate decrease with the addition of 12-13% chromium. However, the corrosion rate is high even at higher chromium and molybdenum contents due to the presence of deleterious phases that locally reduce chromium and molybdenum in solid solution.
Duplex stainless steels show low corrosion rates owing to their high content of chromium and molybdenum. However, the behavior is influenced by the specific microstructures and

the onset of selective attack on austenitic phase, due to the lower amount of chromium and molybdenum than the ferritic one.
Significant weight loss was only observed on nickel alloys for compositions with 20% chromium, but without any molybdenum additions.
Titanium alloys were in any case immune to general corrosion, confirming the well-known good behavior in acidic chloride-containing solutions, due to the formation of stable and protective oxide.

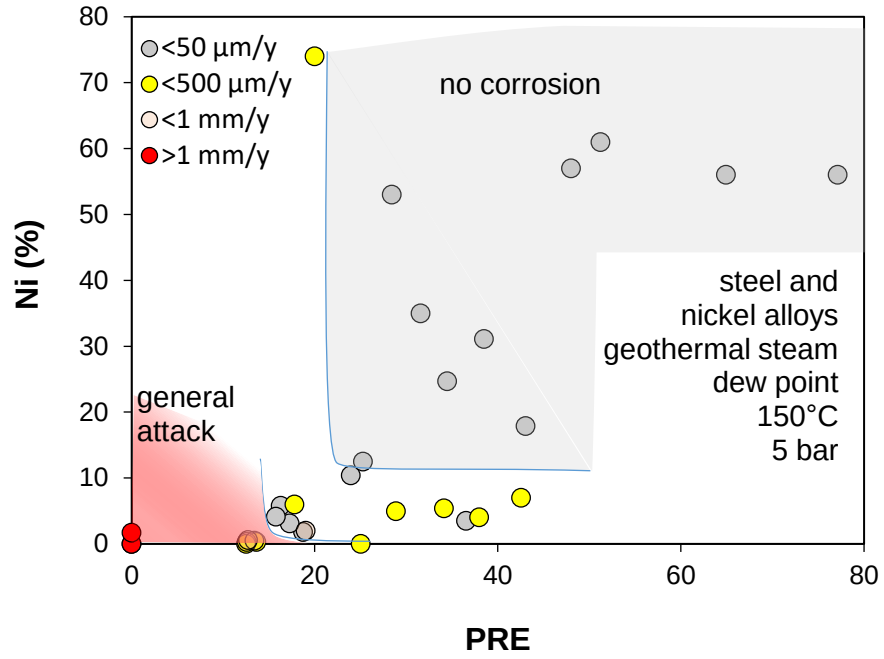

Figure 3: weight loss as a function of pitting resistance equivalent number and nickel content of steels and nickel alloys at the dew point in geothermal plant of Tuscany

3.4 Localized corrosion

Pitting can occur due to the high corrosivity of acid condensates, the presence of very high chloride content and high temperature. Under these environmental conditions, chlorides can induce the breakdown of passive film even on corrosion resistant alloys.
The resistance to localized corrosion of stainless steels and nickel alloys is related to the stability of the passivity against the action of chlorides, that is well addressed by the PRE number.
There are several formulations for PRE, with slightly different coefficients for molybdenum and nitrogen. Some of them also consider the secondary effect of other elements e.g. W and Nb. However, the equation (1) is the most used for stainless steels and it is applied to nickel alloys containing chromium and molybdenum.
Figure 4 shows the critical field for pitting corrosion as a function of PRE number and nickel content. Localized corrosion did never occur during tests on austenitic alloys with pitting index above 38. The duplex alloys showed complex behavior due to occurrence of selective corrosion on improper microstructures.
The results are applicable only to pitting corrosion, since deposits do not form on the surface of specimens during testing.
It can be noted that the localized attack takes place much more easily under deposits. Crevice corrosion has common aspects with pitting but it occurs in less corrosive

environment and requires greater corrosion resistance for its prevention, i.e. stainless steel and nickel alloy with higher PRE index.
Tests confirms the good behavior of all titanium alloys regardless their composition. Localized corrosion was never observed on the specimens. However, it should be noted that the experimental conditions only allow the evaluation of pitting corrosion, as mentioned before. It is well known that titanium alloys show susceptibility to crevice corrosion in reducing acid chloride solutions at temperatures above 80 °C. The guidelines for preventing corrosion phenomena on titanium in reducing environments suggest that it is advisable the use of alloys with a composition capable of ensuring a correct film formation and stable passivity under these conditions [11]. Thus, ELI alloy with addition of ruthenium (grade 29) or alloy with the addition of molybdenum (alloy 6246) are expected to perform better than the most commonly used Ti6Al4V alloy.

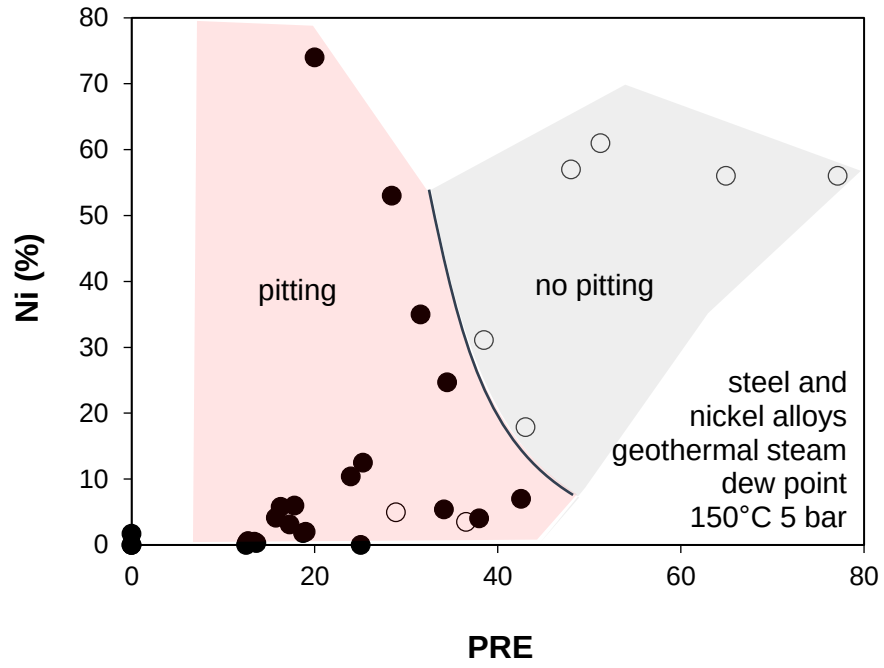

Figure 4: effect of pitting resistance equivalent number and nickel content on the susceptibility of steels and nickel alloys to pitting corrosion at the dew point of geothermal fluid of Tuscany

3.5 Stress corrosion cracking

Stress corrosion cracking results from the synergistic action of tensile stress and corrosion on susceptible alloys.
The susceptibility of austenitic stainless steels and nickel alloys to this form of corrosion in concentrated acidic chloride solutions is well known. It primarily depends on the content of nickel. Actually, nickel-free ferritic and martensitic stainless steels, low-alloy steels and titanium alloys are not susceptible to chloride SCC.
The cracking frequently initiates from pitting attacks, because pits acts as intensifier, promoting high level of stress at the tip. Moreover, the occluded cell locally increases the acidity of the solution and the concentration of chlorides, giving more critic conditions that enhance the risk of cracking.
The attack occurs above 60°C, whereas at low temperature it can occur only on sensitized alloys, susceptible to intergranular corrosion (IGSCC).

Figure 5 shows the results collected on U-bend specimens. SCC was only detected for intermediate nickel contents- between 2% and about 30% - and on alloys with a low PRE index. However low PRE alloys are not suitable due to the occurrence of localized corrosion at the dew point (see previous paragraph). Data in Figure 5 and Figure 4 shows same PRE values that limit the field of critical compositions for pitting and SCC, for nickel content ranging from 10 to 40%. The results confirm the immunity to chloride stress corrosion cracking of Titanium alloys, low-alloyed steels, martensitic and ferritic stainless steels, without any addition of nickel (Figure 9).
In the absence of data obtained directly from the experimentation, the critical range of nickel content for stress corrosion identified in Figure 5 was limited to the values of content normally indicated for immunity of nickel alloys to this form of corrosion. This limit tends to increase with the temperature between 30% and 50% nickel [13].

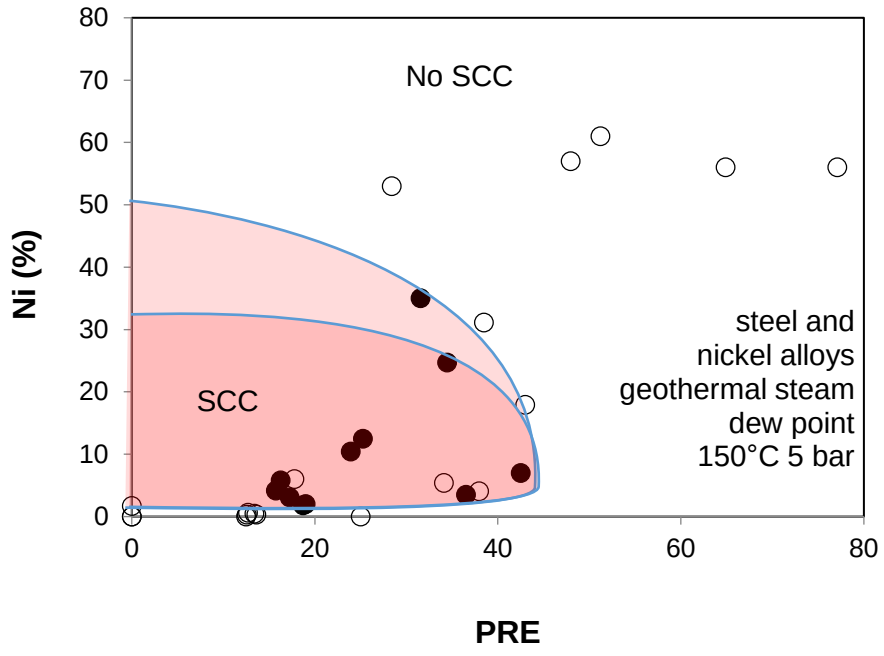

Figure 5: effect of pitting resistance equivalent number and nickel content on the susceptibility of steels and nickel alloys to stress corrosion cracking at the dew point of geothermal fluid of Tuscany

4 Conclusions

The analysis of the results collected on steels, stainless steels, nickel alloys and titanium alloys exposed at the dew point of geothermal fluids of the Larderello geothermal wells allowed to obtain useful data to characterize the behavior to generalized corrosion, pitting and stress corrosion cracking.
The composition of solutions that forms in the early stages of condensation in turbine was estimated by calculating the equilibrium, considering adiabatic transformation, from thermodynamic data and average composition of geothermal fluids. The composition is characterized by values of pH and chlorides content around 3.5 and 6500 ppm, respectively.
Weight loss was negligible in austenitic alloys with nickel content greater than or equal to 10% and the PRE above 20.
The pitting corrosion did never occur on austenitic alloys with pitting index greater than 38.

Stress corrosion cracking was only recognized for intermediate content of nickel, between 2% and about 30%, and on alloys with PRE index below the critical limit observed for pitting corrosion. Tests confirms the good behavior of all titanium alloys regardless their composition. The use of ELI alloys with ruthenium or molybdenum is advised to achieve the formation of a stable passive film also in reducing environments.
The result of tests on stainless steels and nickel alloys are presented as a function of the chemical composition of the alloy, considering the nickel content and the PRE index, in order to obtain susceptibility maps. The maps can be used in order to evaluate limits of compositions for developing material selection criteria for part of geothermal plants in contact with fluids similar to that considered during the experimentation.

5 References

[1] S. Hjartarson, G. Sævarsdóttir, H. Pálsson, K. Ingason, B. Pálsson e W. Harvey, Utilization of chloride bearing, superheated steam, SGP-TR-194, in Thirty-Seventh Workshop on Geothermal Reservoir Engineering, Standford, 2012.

[2] G. Culivicchi, R. Perini, B. Tarquini e A. Lenzi, Corrosion rates in the dew-point zone of supercritic superheated steam, in World Geothermal Congress , Kyushu –Tohoku, Japan, June 2000.

[3] G. Allegrini e G. Benvenuti, Corrosion characteristics and geothermal power plant protection, Geothermics, Vol. 1, Special Issue 2, Part I, n. 2, pp. 2462-2466, 1970.

[4] M. Bracaloni, G. Culivicchi e B. Fornari, Erosion and corrosion problems experienced during the operation of geothermal turbines in Italy, in World Geotheermal Congress, Firenze, 1995.

[5] P. Hirtz, C. Buck e R. Kunzman, Current Techniques in Acid-Chloride Corrosion Control and Monitoring at The Geysers, SGP-TR- 134, in Sixteenth Workshop on Geothermal Reservoir Engineering, Stanford, 1991.

[6] T. Marshall e W. R. Braithwaite, Corrosion control in geothermal systems,, in Geothermal Energy, H. Christopher e H. Armstead, A cura di, Unesco, 1973, pp. 151-160.

[7] A. Paglianti, E. Viviani, E. Brunazzi e F. Sabatelli, A simple method to compute hydrogen chloride abatement in geothermal power plants, Geothermics, vol. 25, n. 1, pp. 37-62, 1996.

[8] J. M. Simonson e D. A. Palmer, Production and mitigation of acid chlorides in geothermal steam, in CONF-950388—2, 1995.

[9] E. Viviani, A. Paglianti, F. Sabatelli e B. Tarquini, Abatement of hydrogen chloride in geothermal power plants, in World Geothermal Congress, 1995.

[10] D. Gallup e J. R. Farison, Testing of materials in corrosive wells at the Geysers geothermal field, in 20th NZ Geothermal Workshop, 1998.

[11] R. Thomas, Titanium in the geothermal industry, Geothermics, vol. 32, p. 679–687, 2003.

[12] Y. Yang, T. Zhang, Y. Yawei Shao, G. Meng e F. Wang, In situ study of dew point corrosion by electrochemical measurement, Corrosion Science, vol. 71, p. 62–71, 2013.

[13] R. H. Johnes, Stress Corrosion Cracking: Material Performance and Evaluation, in Materials Performance and Evaluation, Materials Park, ASM, 1992.

- General corrosion, pitting and stress corrosion cracking characterization of a large number of stainless steel, nickel alloys and titanium alloys
- Material selection criteria for geothermal energy production
- Definition corrosion susceptibility maps for corrosion resistant alloys and titanium alloys